Anal. Chem. **2000,** *72,* 2609−2612

X-ray Raman Spectroscopy of Carbon in Asphaltene: Light Element Characterization with Bulk Sensitivity

Uwe Bergmann,[†] Oliver C. Mullins,[‡] and S. P. Cramer*,[†,§]

Physical Biosciences Division, Lawrence Berkeley National Laboratory, Berkeley, California 94720, Schlumberger-Doll Research, Ridgefield, Connecticut 06877, and Department of Applied Science, University of California, Davis, California 95616

X-ray Raman spectra of the carbon K-edge have been recorded using 6.461 keV radiation for a petroleum asphaltene. By comparison with coronene, graphite, and paraffin standards, the asphaltene spectrum is seen to be composed of contributions from saturated and aromatic carbon species. The information contained in the carbon K-edge was extracted with bulk (∼1 mm) sensitivity, because the Raman method used hard X-rays. This helps alleviate concerns about surface artifacts that frequently occur with soft X-ray spectroscopy of light elements. X-ray Raman spectroscopy shows great potential for characterization of light elements in fuels, catalysts, and other complex materials under chemically relevant conditions.

Asphaltenes are complex mixtures of heteroatom-rich aromatic hydrocarbons that are present as a solid suspension in crude oils.[1−4] Asphaltenes dramatically affect the chemical and physical properties of crude oils, and they limit the range of processes that can be utilized. Optimal exploitation of crude oil resources requires a thorough knowledge of chemical and physical properties of asphaltenes, yet due to their complexity and heterogeneity, these materials have resisted precise characterization.

Even such fundamental issues as molecular weight and structure have proven controversial. Of particular interest are the average number and distribution of the number of fused rings within asphaltene molecules. ^{13}C NMR can quantitate the aromatic-to-saturated carbon ratio, but it does not establish the size of the aromatic ring systems. Initial estimates for the number of fused benzene rings varied widely, from 4 rings to 25 rings.[2,3] An average of seven rings has been derived from NMR[5] and from optical spectroscopy.[3,6] More recently, these ring number estimates have been supported by scanning tunneling microscopy measurements[7] and measurements of molecular rotation dynamics by fluorescence depolarization.[8] Molecular weights found in field desorption mass spectroscopy[9] and laser desorption mass spectroscopy[10] support this number of fused rings.

Carbon K-edge X-ray absorption near-edge spectroscopy (XANES) appears promising as a technique for probing the speciation of carbon in asphaltenes. An important advantage of this technique is that it probes all chemical forms of the element in question. The carbon K-edge exhibits 1s → π^* and 1s → σ^* XANES transitions which are sensitive to the degree of unsaturation and to the carbon−neighbor bond lengths.[11] K-edge measurements have already been successfully employed to characterize the sulfur[4,12−14] and nitrogen[4,15,16] in asphaltenes and coals. However, one potential problem for carbon K-edge spectroscopy is that it involves a low-energy "soft" X-ray that has an attenuation length of ∼0.1 μm.

In most cases, it is impractical to prepare the homogeneous submicrometer-thick samples required for transmission experiments at the carbon K-edge. Fluorescence detection is also not appropriate for quantitative measurements of carbon in fuels, since the samples are neither "dilute" nor "thin", and saturation effects would be significant in excitation spectra.[17] Thus, in this spectral region, it is common to employ sample photocurrent or electron yield detection methods.[11] These techniques have typical probe depths of ∼50 Å.[18]

[†] Lawrence Berkeley National Laboratory.

[‡] Schlumberger-Doll Research.

[§] University of California, Davis.

(1) Chilingarian, G. V.; Yen, T. F. In *Bitumens, asphalts and tar sands*; Chilingarian, G. V., Yen, T. F., Eds.; Elsevier Scientific: New York, 1978.
(2) Speight, J. G. *The chemistry and technology of petroleum*; Marcel Dekker: New York, 1980.
(3) Mullins, O. C.; Sheu, E. Y. In *Structures and dynamics of asphaltenes*; Mullins, O. C., Sheu, E. Y., Eds.; Plenum Press: New York, 1998.
(4) Sheu, E. Y.; Mullins, O. C. In *Asphaltenes, fundamentals and applications*; Sheu, E. Y., Mullins, O. C., Eds.; Plenum: New York, 1995.
(5) Calemma, V.; P. Iwanski, P.; Nali, M.; Scotti, R.; Montanari, L. *Energy Fuels* **1995**, *9*, 225.
(6) Ralston, C. Y.; Mitra-Kirtley, S.; Mullins, O. C. *Energy Fuels* **1996**, *10*, 623.
(7) Zajac, G. W.; Sethi, N. K.; Joseph, J. T. *Scanning Microsc.* **1994**, *8*, 463.
(8) Groenzin, H.; Mullins, O. C. *J. Phys. Chem., A* **1999**, *103*, 11237−11245.
(9) Boduszynski, M. M. *Energy Fuels* **1988**, *2*, 597.
(10) Miller, J. T.; Fisher, R. B.; Thiyagarajan, P.; Winans, R. E.; Hunt, J. E. *Energy Fuels* **1998**, *12*, 1290.
(11) Stöhr, J. *NEXAFS Spectroscopy*; Springer-Verlag: New York, 1992.
(12) George, G. N.; Gorbaty, M. L. *J. Am. Chem. Soc.* **1989**, *111*, 3182.
(13) Huffman, G. P.; Mitra, S.; Huggins, F. E.; Shah, N.; Vaidya, S.; Lu, F. *Energy Fuels* **1991**, *5*, 574.
(14) Waldo, G. S.; Mullins, O. C.; Penner-Hahn, J. E.; Cramer, S. P. *Fuel* **1992**, *71*, 53.
(15) Mitra-Kirtley, S.; Mullins, O. C.; van Elp, J.; George, S. J.; Chen, J.; Cramer, S. P. *J. Am. Chem. Soc.* **1993**, *115*, 252−258.
(16) Mullins, O. C.; Mitra-Kirtley, S.; van Elp, J.; Cramer, S. P. *Appl. Spectrosc.* **1993**, *47*, 1268−1275.
(17) Goulon, J.; Goulon-Ginet, C.; Cortes, R.; Dubois, J. M. *J. Phys.* **1982**, *43*, 539−548.
(18) Abbate, M.; Goedkoop, J. B.; deGroot, F. M. F.; Grioni, M.; Fuggle, J. C.; Hofmann, S.; Petersen, H.; Sacchi, M. *Surf. Interface Anal.* **1992**, *18*, 65−69.

10.1021/ac990730t CCC: $19.00
Published on Web 04/21/2000

The shallow probe depth for electron detection methods is often a concern. Surface oxidation is facile in carbonaceous materials, and various molecules are expected to adsorb to or selectively migrate to the surface region. Differences between surface and bulk compositions of coals for sulfur[19] and nitrogen[20] have been observed. Furthermore, both electron detection and soft X-rays make it difficult to use windows that would maintain natural or reactive environments around a sample. Thus, a hard X-ray method for carbon analysis with bulk sensitivity would be especially valuable. X-ray Raman spectroscopy is just such a technique.

In an X-ray Raman measurement, the incident photon is inelastically scattered and a fraction of the energy is transferred to the sample. Some events correspond to the vibrational excitations familiar with UV−visible Raman spectroscopy. However, since the incident photon energy is in the kiloelectronvolt range and vibrational energies are typically 4−5 orders of magnitude smaller (10−500 meV), extremely high resolution is required for vibrational X-ray Raman spectroscopy.[21−23] X-ray Raman spectroscopy can also probe electronic excitations in the 1−10 eV range that are normally the domain of UV−visible and near-infrared spectroscopy. For example, soft X-ray resonance fluorescence has been used to monitor d−d and charge-transfer excitations in transition metal and rare earth compounds such as MnO,[24] CeO_2,[25] PrO_2,[26] and copper oxides.[27] Hard X-ray experiments have probed charge-transfer excitations in NiO[28] and Nd_2CuO_4[29] and quadrupolar transitions in Gd.[30]

The high energy of hard X-ray photons also permits electronic excitation of core levels in the sample. This means that one can effectively measure soft X-ray absorption spectra using hard X-rays. In 1967, Mizuno and Ohmura showed that the transition probability for X-ray Raman scattering can be related to the same dipole matrix element that determines X-ray absorption.[31] For a powder sample, the transition probability for scattering, w, is described by[32]

$$w = \{(4\pi^3 e^4 h)/(m^2 \nu_i \nu_j)\}(1 + \cos^2\theta)\, |\langle f|\exp(iqr)|i\rangle|^2 \delta(E_f - E_0 - h(\nu_i - \nu_j))$$

where $\langle f|$ and $|i\rangle$ are the final and initial state wave functions, ν_i and ν_j are incident and scattered X-ray frequencies, θ is the scattering angle, and q is the momentum transfer. When $qr \ll 1$, the dipole approximation is valid and (also using $|k_i| \cong |k_j|$) the above equation becomes[32]

$$w = \{(64\pi^5 e^4 h)/(m^2 c^2)\}(1 + \cos^2\theta)\sin^2(\theta/2)|\langle i|r|f\rangle|^2$$

where the matrix element is the same as for dipole X-ray absorption.[31] However, when q is large, the appearance of the spectrum can change because of the contribution from nondipole terms. This effect has been demonstrated in the spectrum of lithium metal.[33]

The predicted correspondence between X-ray Raman and soft X-ray absorption was observed more than 30 years ago.[34] However, because of the small cross section for Raman scattering and the need for a scattered beam analyzer, X-ray Raman has remained a difficult experiment. The pioneering Suzuki experiments used a flat LiF(200) crystal, and they achieved Raman rates of <1 photon/s with a rotating anode source and >10 eV resolution.[34] Tohji and Udagawa achieved ~100-fold higher signal rates and 6 eV resolution using a synchrotron radiation source, a cylindrically bent Ge(333) analyzer, and a position-sensitive detector.[32,35] In other synchrotron-based studies, Watanabe and co-workers a used cylindrically bent Ge(440) crystal and position-sensitive detector to obtain spectra in a few hours with 1.5 eV resolution.[36] A resolution of 0.8 eV was reported by Schülke and co-workers using a spherically bent Si(444) analyzer,[37] while Krisch and co-workers achieved better than 0.2 eV resolution in their Raman study of the lithium K-edge.[33]

For this current study, we used an array of spherically bent Si crystals to capture a larger solid angle. We report the carbon Raman XANES spectra of an asphaltene sample along with those of graphite, paraffin, and coronene model compounds. The features in the model compound spectra are discussed and compared with known soft X-ray absorption spectra. The asphaltene spectrum is quantitatively analyzed in terms of the model compound spectra.

EXPERIMENTAL SECTION

The experiments were performed at the National Synchrotron Light Source (NSLS) wiggler beamline X-25 using a Si(111) double-crystal monochromator and the vertical focusing mode.[38] The Raman scattering was analyzed with our high-resolution multicrystal spectrometer. The instrument employs eight Si(440) analyzer crystals on intersecting Rowland circles, and a detailed description is available.[39] To obtain the best energy resolution,

(19) Perry, D. L.; Grint, A. *Fuel* **1983**, *62*, 1029.
(20) Kelemen, S. R.; Gorbaty, M. L.; Kwiatek, P. J. *Energy Fuels* **1994**, *8*, 896.
(21) Masciovecchio, C.; Bergmann, U.; Krisch, M.; Ruocco, G.; Sette, F.; Verbeni, R. *Nucl. Instrum. Methods B* **1996**, *111*, 181−186.
(22) Verbeni, R.; Sette, F.; Krisch, M. H.; Bergmann, U.; Gorges, B.; Halcoussis, C.; Martel, K.; Masciovecchio, C.; Ribois, J. F.; Ruocco, G.; Sinn, H. *J. Synchrotron Radiat.* **1996**, *3*, 62−64.
(23) Sette, F.; Ruocco, G.; Krisch, M.; Bergmann, U. *Phys. Rev. Lett.* **1995**, *75*, 850−853.
(24) Butorin, S. M.; Guo, J.-H.; Magnuson, M.; Kuiper, P.; Nordgren, J. *Phys. Rev. B* **1996**, *54*, 4405−4408.
(25) Butorin, S. M.; Mancini, D. C.; H., G. J.; Wassdahl, N.; J., N. *J. Alloys Compd.* **1995**, *225*, 230−233.
(26) Butorin, S. M.; Duda, L.-C.; Guo, J.-H.; Wassdahl, N.; Nordgen, J. *J. Phys.: Condensed Matter* **1997**, *9*, 8155−8160.
(27) Guo, J. H.; N., W.; P., S.; S., B.; Nordgren, J. *J. Phys. Chem. Solids* **1993**, *54*, 1203−1206.
(28) Kao, C.-C.; Caliebe, W. A. L.; Hastings, J. B.; Gillet, J.-M. *Phys. Rev. B* **1996**, *54*, 16361−16364.
(29) Hill, J. P.; Kao, C. C.; Caliebe, W. A. L.; Matsubara, M.; Kotani, A.; Peng, J. L.; Greene, R. L. *Phys. Rev. Lett.* **1998**, *80*, 4967−4970.
(30) Krisch, M. H.; Kao, C. C.; Sette, F.; Caliebe, W. A.; Others., A. *Phys. Rev. Lett.* **1995**, *74*, 4931−4934.
(31) Mizuno, Y.; Ohmura, Y. *J. Phys. Soc. Jpn.* **1967**, *22*, 445.
(32) Tohji, K.; Udegawa, Y. *Phys. Rev. B* **1989**, *39*, 7590−7594.
(33) Krisch, M. H.; Sette, F.; Masciovecchio, C.; Verbeni, R. *Phys. Rev. Lett.* **1997**, *78*, 2843−2846.
(34) Suzuki *J. Phys. Soc. Jpn.* **1967**, *22*, 1139.
(35) Tohji, K.; Udegawa, Y. *Phys. Rev. B* **1987**, *36*, 9410−9412.
(36) Watanabe, N.; Hayashi, H.; Udagawa, Y.; Takeshita, K.; Kawata, H. *App. Phys. Lett.* **1996**, *69*, 1370−1372.
(37) Schülke, W.; Bonse, U.; Nagasawa, H.; Kaprolat, A.; Berthold, A. *Phys. Rev. B* **1988**, *38*, 2112−2123.
(38) Berman, L. E.; Hastings, J. B.; Oversluizen, T.; Woodle, M. *Rev. Sci. Inst.* **1992**, *63*, 428−432.
(39) Bergmann, U.; Cramer, S. P. *Proc. SPIE-Int. Soc. Opt. Eng.* **1998**, *3448*, 198−209.

the instrument was tuned as close as possible to backscattering, which in our setup corresponded to a Bragg angle $\theta_B = 88°$ and an energy of 6461 eV. In this geometry, the analyzer energy resolution is estimated to be ~0.5 eV. The Raman spectrum is swept by scanning the beamline monochromator energy, and the line width of the excitation beam contributes to the overall width of the spectra. The overall energy resolution was found to be 2 eV fwhm by measuring the elastic scattering peak.

The scattered intensity was measured with a NaI detector which was shielded with lead foil to reduce the background. A 3 × 15 mm entrance slit in the shielding allowed the monochromated photons to reach the detector. The incident flux (I_0) was recorded with an air-filled ion chamber, and the spectra were corrected for changes in I_0 resulting from ring current decay and monochromator heating. The Raman spectrum was also corrected for the background from Compton scattering, by subtracting an extrapolated polynomial of the arbitrary form, $a^*(E - b) + c + d/(E - e)$, where E is the photon energy and the terms are fitted parameters.

The incident beam intensity was on the order of order 6×10^{11} photons/s in a 1 mm vertical by 2 mm horizontal beam spot. Individual scans took 30 min with 5 s per step. The step size varied from 10 eV far below the edge to 0.25 eV at the edge to 1−10 eV in the region above the edge. To obtain similar statistics, the data collection time was varied depending on the Raman signal. The number of scans recorded was 4 for graphite, 5 for paraffin, 8 for coronene, and 10 for the asphaltene. The samples were at room temperature in air during data collection. Although beam damage might be significant at higher fluxes or over longer acquisition times, we saw no evidence that the spectra were changing from one scan to the next.

The asphaltene was prepared from a Kuwait crude oil (UG8) using *n*-heptane precipitation as described previously.[15] Coronene, paraffin, and KS-10 synthetic graphite were obtained from Aldrich and used without further purification.

RESULTS AND DISCUSSION

Figure 1 shows a comparison between our Raman mode spectrum for graphite versus a soft X-ray absorption spectrum for the same material taken in electron yield mode.[40] Similar graphite absorption spectra have been reported before.[41,42] In both absorption and Raman spectra, there is a strong resonance at ~285 eV. This is a 1s → π^* transition that is a characteristic signature of π-bonding in a sample.[11] Another strong feature occurs at 292 eV—this is a primarily a 1s → σ^* feature, corresponding to electronic transitions polarized along the C−C axis.[43] Schülke and co-workers have shown that the 285 eV resonance is polarized parallel to the graphite *c*-axis, as expected for a 1s → π^* transition, while the higher energy feature is enhanced with momentum transfer $q \perp c$.[37] At still higher energies, there are XANES features that correspond to multiple scattering events between different shells of neighbors, and the spectrum gradually transforms into the longer range EXAFS oscillations. Apart from the broadening due to lower energy resolution, there is a good agreement between Raman and absorption spectra in the energy and relative intensity of spectral features. This close correspondence helps support the assumption that our X-ray Raman spectra are representative of the carbon K-edge XANES.

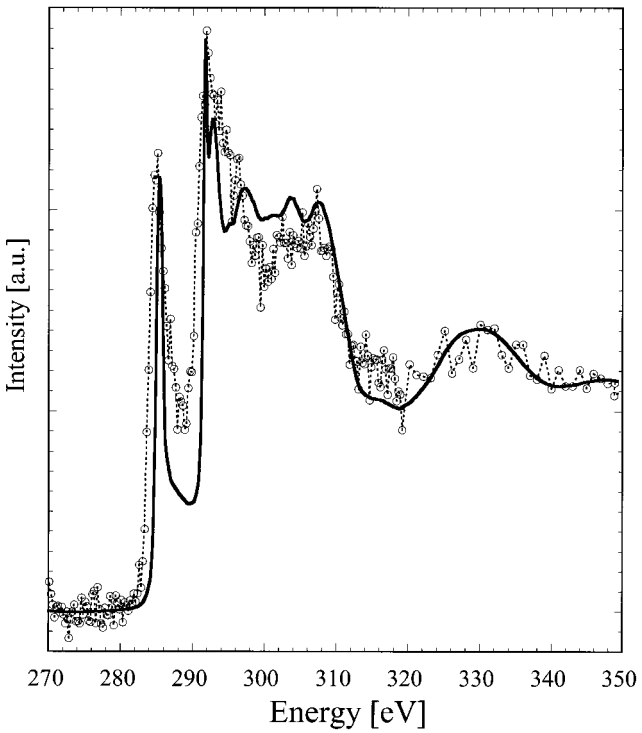

Figure 1. Comparison of graphite carbon K-edge spectra obtained (a) as soft X-ray absorption spectrum using electron yield (solid line) and (b) by Raman scattering with hard X-rays (open circles and dashed line).

Figure 2 shows the carbon Raman spectra for paraffin, coronene, and the asphaltene sample. The spectrum of the paraffin shows a sharp edge with a shoulder at ~288 eV and the main 1s → σ^* resonance at ~293 eV. In contrast, the coronene shows a 1s → σ^* resonance at about the same energy, as well as a feature at ~285 eV. On the basis of assignments of other unsaturated carbon compounds,[43] this corresponds to a 1s → π^* transition.

The asphaltene exhibits a more diffuse Raman spectrum, which is not surprising considering the complex mixture of molecules involved in this sample. Nevertheless, low-energy structure can be distinguished in this spectrum that clearly represents 1s → π^* intensity. The intensity of this feature can be used to estimate the aromatic fraction of the carbon in this asphaltenes, assuming that the model compounds represent accurate spectral models for the saturated and aromatic components of asphaltenes. In this regard, we note that coronene has seven aromatic rings, and it has the type of structure expected for the aromatic asphaltene component. A fit to the entire XANES region (282−320 eV) suggests a mixture of 50% aromatic and 50% saturated carbon. Of course, the use of only two model compounds makes these numbers only suggestive, not quantitative. Furthermore, Schülke and co-workers have shown that, in Raman mode, there is a q dependence to the relative intensity of different features,[37] and this angular sensitivity must be addressed in any quantitative analysis.

(40) Anders, S.; Diaz, J.; Ager III, J. W.; Lo, R. Y.; Bogy, D. B. *App. Phys. Lett.* **1997**, *7*, 3367−3369.
(41) Denley, D.; Perfetti, P.; Williams, R. S.; Shirley, D. A.; Stöhr, J. *Phys. Rev. B* **1980**, *21*, 2267−2273.
(42) Comelli, G.; Stöhr, J.; Jark, W.; Pate, B. B. *Phys. Rev. B* **1988**, *37*, 4383−4389.
(43) Bianconi, A. In *XANES Spectroscopy*; Bianconi, A., Ed.; Wiley-Interscience: New York, 1988; pp 573−662.

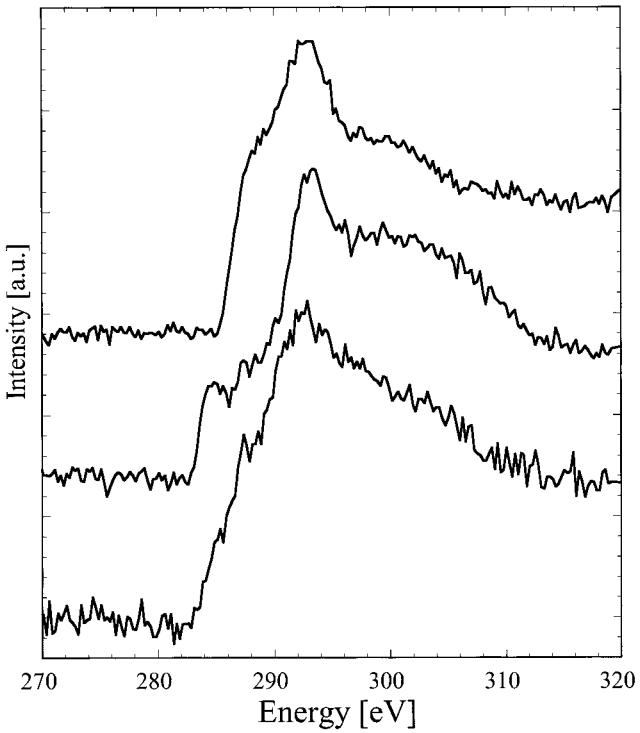

Figure 2. Comparison of carbon XANES obtained using the Raman technique for paraffin (top), coronene (middle), and asphaltene (bottom). Spectra have been background corrected and normalized to yield the same edge jump.

Despite these limitations, the Raman mode carbon XANES spectrum of asphaltenes can be used to exclude certain types of aromatic structures. For example, the preedge region of graphite (Figure 1) exhibits a sharp resonance that is quite different from that of coronene or the asphaltene. The 1s → π^* resonances in C-60 and in C-70 are also much larger and lower in energy than in the asphaltene. It probably comes as no surprise that the carbon XANES spectrum shown here is incompatible with the presence of graphitic or C-60 carbon in asphaltenes. However, with a broader model compound base, in the future it may be possible to exclude the presence of other ring systems. This is currently under investigation.

SUMMARY AND CONCLUSIONS

We have shown that carbon XANES obtained in the X-ray Raman mode can be used to help characterize complex materials such as asphaltenes. From the relative intensity of 1s → π^* and 1s → σ^* resonances, we estimate the fraction of aromatic in the asphaltene to be ~50%. The energy of the 1s → π^* transition is consistent with other reports indicating that the asphaltene aromatic moieties contain on the order of seven fused rings.

The Raman technique avoids the surface sensitivity of soft X-ray absorption spectroscopy and is, thus, less sensitive to problems such as surface oxidation or contamination. Problems with surface sensitivity have limited the potential of conventional soft X-ray methods for the study of asphaltenes, fuels, and other reactive materials. Future work will focus on collecting a larger set of model spectra to address the identity of aromatic moieties in asphaltenes, as well as using third-generation synchrotron sources to obtain even better spectral resolution.

ACKNOWLEDGMENT

We thank Dr. Simone Anders for providing the graphite electron yield spectrum. This research was supported by the National Institutes of Health, Grants 44891-5 and GM-48145 (to S.P.C.) and by the Department of Energy, Office of Biological and Environmental Research. The National Synchrotron Light Source and the Advanced Light Source are supported by the Department of Energy, Office of Basic Energy Sciences.

Received for review July 2, 1999. Accepted February 11, 2000.

AC990730T